

p-Anisaldehyde as a Ligand in Molybdenum and Tungsten Complexes: σ or π ?

D. M. Schuster, P. S. White, and J. L. Templeton*

W. R. Kenan, Jr., Laboratories, Department of Chemistry, University of North Carolina, Chapel Hill, North Carolina 27599-3290

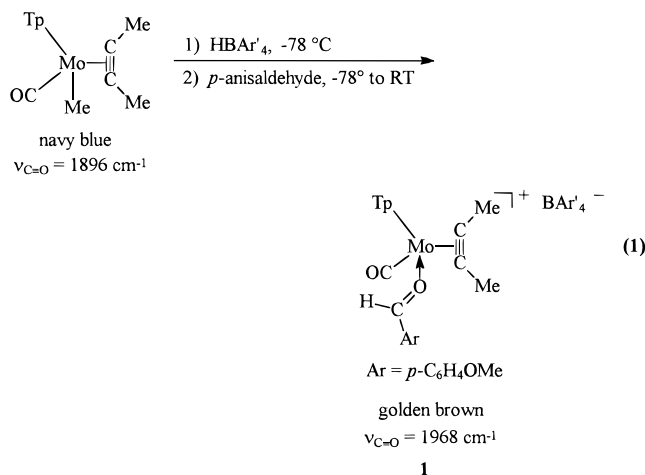
Received October 14, 1996[®]

Summary: The different binding modes of *p*-anisaldehyde to the [TpMo(CO)(MeC≡CMe)]⁺ and [TpW(CO)(MeC≡CMe)]⁺ fragments in solution have been assessed by IR and ¹H and ¹³C NMR spectra. X-ray analyses substantiate that *p*-anisaldehyde is σ -bound in the molybdenum complex **1** and π -bound in the tungsten complex **2**.

The reactivity of aldehydes and ketones bound to transition-metal Lewis acids has been investigated extensively.^{1–3} These studies reveal the influence of ancillary ligands and type of organic carbonyl on the mode of coordination of bound aldehydes and ketones. In contrast, few examples directly probe the impact of the metal.⁴ Herein, we report coordination of *p*-anisaldehyde to the TpMo(CO)(MeC≡CMe)⁺ and TpW(CO)(MeC≡CMe)⁺ (Tp = hydridotripyrazolylborate) metal fragments. The aldehyde and ancillary ligands are constant in the two systems, isolating the metal as the sole discriminating factor for the mode of aldehyde coordination.

Protonation of the navy blue methyl complex TpMo(CO)(MeC≡CMe)Me ($\nu_{C=O}$ 1896 cm⁻¹) with HBAR'₄·2OEt₂ (BAR'₄ = tetrakis[3,5-bis(trifluoromethyl)phenyl]borate)⁵ in CH₂Cl₂ at -78 °C followed by addition

of *p*-anisaldehyde and subsequent warming to ambient temperature yields a golden brown solution of [TpMo(CO)(MeC≡CMe)(η^1 -*p*-O=CHC₆H₄OMe)][BAR'₄] (**1**; $\nu_{C=O}$ 1968 cm⁻¹), as shown in eq 1.⁶ NMR signals at 8.30 ppm



(CHO) in the ¹H spectrum and 197.2 ppm (CHO) in the ¹³C spectrum are diagnostic for an η^1 -*p*-anisaldehyde complex.^{1a,7} Broad *ortho* and *meta* aryl carbon resonances in the ¹³C NMR spectrum (135.0, 115.9 ppm) reflect restricted rotation about the aryl-carbonyl carbon bond due to π -delocalization from the electron-rich aryl group to the aldehyde functionality.⁸ At -80 °C the aryl rotation has slowed and four separate aryl signals are observed (137.5, 131.4, 116.3, 112.8 ppm). The aldehyde carbonyl resonance (-80 °C: CHO, 195.6 ppm) in ¹³C NMR and the aldehydic proton resonance (-80 °C: CHO, 8.02 ppm) in ¹H NMR are shifted only slightly from ambient-temperature values, indicating that the aldehyde maintains its σ mode of coordination at low temperatures.

Workup of **1** gave emerald green crystals in 81% yield. An X-ray crystal structure determination substantiates the η^1 -coordination of *p*-anisaldehyde to the octahedral molybdenum metal center (Figure 1). The molecule adopts the sterically less demanding *E* conformation about the C=O bond³¹ with a Mo(1)-O(5)-C(6) bond angle of 144.0(4)°. An O(5)-C(6)-C(11) angle of 122.2-(6)° is consistent with sp² hybridization at the carbonyl (CHO) carbon. The C=O bond length (1.237(7) Å) is similar to the length in other structurally characterized

(6) [TpMo(CO)(MeC≡CMe)(η^1 -*p*-O=CHC₆H₄OMe)][BAR'₄] (**1**): IR (CH₂Cl₂) $\nu_{C=O}$ 1968 cm⁻¹; ¹H NMR (200 MHz, CD₂Cl₂) δ 8.30 (s, 1 H, CHO), 7.50, 6.97 (both br d, 2 H each, ³J_{HH} = 9.0 Hz for both, C₆H₄), 3.89 (s, 3 H, OMe); ¹³C{¹H} NMR (400 MHz, CD₂Cl₂, -80 °C) δ 195.6 (CHO), 167.3 (C-OMe of C₆H₄), 137.5, 131.4 (C₆H₄), 125.7 (*ipso* of C₆H₄), 116.3, 112.8 (C₆H₄), 55.9 (OMe).

(7) ¹H NMR for free *p*-anisaldehyde (CD₂Cl₂): δ 9.86 (s, CHO).

(8) A helpful reviewer suggested that this broadening could be due to slow rotation about the MeO-C(*ipso*) bond. Since broadening is seen with coordinated benzaldehyde, restricted rotation about the O=C-C(*ipso*) bond is more likely.

[®] Abstract published in *Advance ACS Abstracts*, November 15, 1996.

(1) For reviews see: (a) Huang, Y. H.; Gladysz, J. A. *J. Chem. Educ.* **1988**, *65*, 298 and references therein. (b) Shambayati, S.; Schreiber, S. L. In *Comprehensive Organic Synthesis*; Trost, B. M., Editor-in-Chief; Fleming, I., Deputy Editor-in-Chief; Schrieber, S. L., Volume Editor; Pergamon: New York, 1991; Vol. 1, Chapter 1.10.

(2) For a theoretical study see: Delbecq, F.; Sautet, P. *J. Am. Chem. Soc.* **1992**, *114*, 2446.

(3) For general leading references see: (a) Boone, B. J.; Klein, D. P.; Seyler, J. W.; Méndez, N. Q.; Arif, A. M.; Gladysz, J. A. *J. Am. Chem. Soc.* **1996**, *118*, 2411. (b) Denmark, S. E.; Almstead, N. G. *J. Am. Chem. Soc.* **1993**, *115*, 3133. (c) Faller, J. W.; Ma, Y. *J. Am. Chem. Soc.* **1991**, *113*, 1579. (d) Williams, D. S.; Schofield, M. H.; Anhaus, J. T.; Schroek, R. R. *J. Am. Chem. Soc.* **1990**, *112*, 6728. (e) Bullock, R. M.; Rappoli, B. J. *J. Am. Chem. Soc.* **1991**, *113*, 1659. (f) Barry, J. T.; Chacon, S. T.; Chisholm, M. H.; Huffman, J. C.; Strieb, W. E. *J. Am. Chem. Soc.* **1995**, *117*, 1974. (g) Sünkel, K.; Urban, G.; Beck, W. *J. Organomet. Chem.* **1985**, *290*, 231. (h) Wang, Y.; Agbossou, F.; Dalton, D. M.; Liu, Y.; Arif, A. M.; Gladysz, J. A. *Organometallics* **1993**, *12*, 2699. (i) Garner, C. M.; Méndez, N. Q.; Kowalczyk, J. J.; Fernández, J. M.; Emerson, K.; Larsen, R. D.; Gladysz, J. A. *J. Am. Chem. Soc.* **1990**, *112*, 5146. (j) Méndez, N. Q.; Seyler, J. W.; Arif, A. M.; Gladysz, J. A. *J. Am. Chem. Soc.* **1993**, *115*, 2323. (k) Foxman, B. M.; Klemarczyk, P. T.; Liptrot, R. E.; Rosenblum, M. *J. Organomet. Chem.* **1980**, *187*, 253. (l) Shambayati, S.; Crowe, W. E.; Schreiber, S. L. *Angew. Chem., Int. Ed. Engl.* **1990**, *29*, 256. (m) Cicero, R. L.; Protasiewicz, J. D. *Organometallics* **1995**, *14*, 4792. (n) Dalton, D. M.; Fernández, J. M.; Emerson, K.; Larsen, R. D.; Arif, A. M.; Gladysz, J. A. *J. Am. Chem. Soc.* **1990**, *112*, 9198. (o) Faller, J. W.; Ma, Y.; Smart, C. J.; DiVerdi, M. J. *J. Organomet. Chem.* **1991**, *420*, 237. (p) Burmeister, J. L. *Coord. Chem. Rev.* **1968**, *3*, 225. (q) Caldarelli, J. L.; Wagner, L. E.; White, P. S.; Templeton, J. L. *J. Am. Chem. Soc.* **1994**, *116*, 2878.

(4) (a) Powell, D. W.; Lay, P. A. *Inorg. Chem.* **1992**, *31*, 3542. (b) Harman, W. D.; Sekine, M.; Taube, H. *J. Am. Chem. Soc.* **1988**, *110*, 2439. (c) Harman, W. D.; Dobson, J. C.; Taube, H. *J. Am. Chem. Soc.* **1989**, *111*, 3061. (d) Harman, W. D.; Fairlie, D. P.; Taube, H. *J. Am. Chem. Soc.* **1986**, *108*, 8223.

(5) (a) Nishida, H.; Takada, N.; Yoshimura, M.; Sonoda, T.; Kobayashi, H. *Bull. Chem. Soc. Jpn.* **1984**, *57*, 2600. (b) Brookhart, M.; Grant, B.; Volpe, A. F. *Organometallics* **1992**, *11*, 3920.

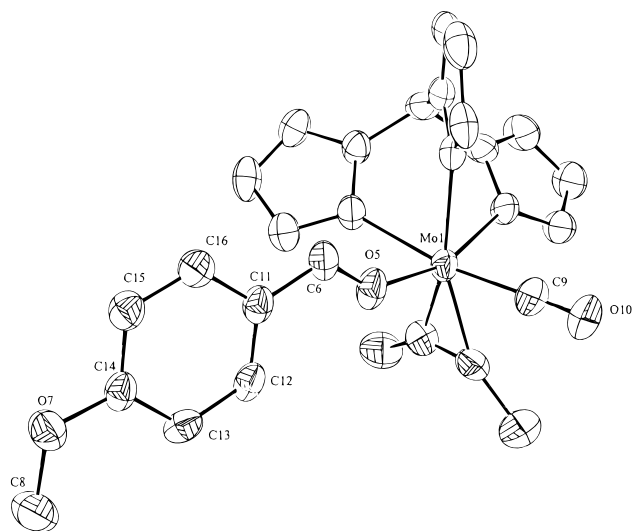


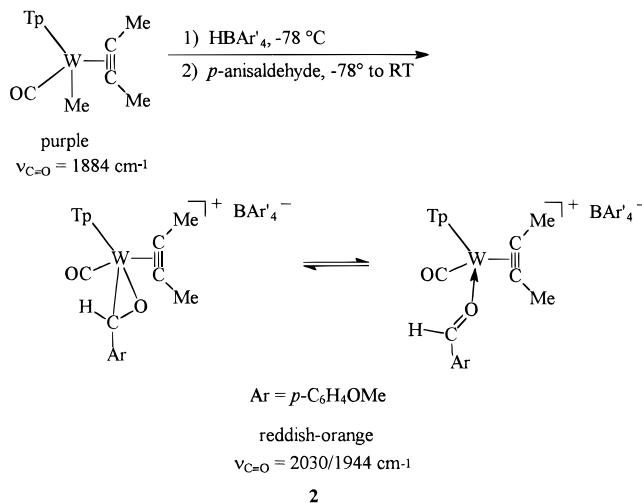
Figure 1. ORTEP diagram for $[\text{TpMo}(\text{CO})(\text{MeC}\equiv\text{CMe})(\eta^1\text{-}p\text{-O}=\text{CHC}_6\text{H}_4\text{OMe})][\text{BAR}'_4]$ (**1**). Selected bond distances (Å) and angles (deg): Mo(1)–C(9), 1.966(6); Mo(1)–O(5), 2.044(4); C(9)–O(10), 1.158(8); O(5)–C(6), 1.237(7); C(6)–C(11), 1.438(8); C(11)–C(12), 1.395(9); C(12)–C(13), 1.372(9); C(13)–C(14), 1.389(8); C(14)–C(15), 1.395(9); C(15)–C(16), 1.365(9); C(16)–C(11), 1.400(8); C(14)–O(7), 1.349(7); O(7)–C(8), 1.439(8); Mo(1)–O(5)–C(6), 144.0(4); O(5)–Mo(1)–C(9), 93.02(22); O(5)–C(6)–C(11), 122.2(6); C(8)–O(7)–C(14)–C(13), 4.6.

$\eta^1\text{-}p\text{-anisaldehyde}$ complexes.^{3j,m,9} The distance between molybdenum and C(6) is 3.131 Å, well beyond the range expected for a π -bound aromatic aldehyde molybdenum complex.¹⁰ The C(8)–O(7)–C(14)–C(13) torsion angle is 4.6°, consistent with extensive conjugation throughout the $p\text{-anisaldehyde}$ ligand.

The $[\text{TpW}(\text{CO})(\text{MeC}\equiv\text{CMe})(\eta^1/\eta^2\text{-}p\text{-O}=\text{CHC}_6\text{H}_4\text{OMe})][\text{BAR}'_4]$ complex (**2**) was prepared by the same method as the molybdenum analogue. The purple $\text{TpW}(\text{CO})(\text{MeC}\equiv\text{CMe})\text{Me}$ complex ($\nu_{\text{C}=\text{O}}$ 1884 cm^{-1}) was protonated with $\text{HBAR}'_4 \cdot 2\text{OEt}_2$ in CH_2Cl_2 at -78°C followed by addition of $p\text{-anisaldehyde}$ and subsequent warming to ambient temperature to generate a reddish orange solution of **2** (Scheme 1).¹¹ The solution IR of **2** at 21 °C reveals both σ - and π -isomers. The tungsten C≡O band for the π -isomer appears 86 cm^{-1} higher than the C≡O band of the σ -isomer (2030 vs 1944 cm^{-1} , respectively), indicating an important back-bonding interaction from tungsten to the C=O π^* orbital of the aldehyde in the π -isomer.

The aldehydic signal in ^1H NMR at ambient temperature (CHO , 7.15 ppm) lies between the values expected for σ - and π -isomers^{1a} and is 1.15 ppm upfield from the $\eta^1\text{-}p\text{-anisaldehyde}$ complex **1**. As with complex **1**, the *ortho* and *meta* carbons of the aryl ring of **2** are broad signals (126.5, 115.1 ppm) in the ^{13}C NMR which decoalesce into four separate signals (-40°C : 131.4,

Scheme 1



125.3, 114.7, 113.8 ppm) at lower temperatures. Due to the dynamic π/σ equilibrium of **2** and the enormous chemical shift difference of the carbonyl carbon (CHO) between π (90–100 ppm) and σ (190–200 ppm) $\text{TpW}(\text{CO})(\text{MeC}\equiv\text{CMe})^+$ aldehyde adducts,¹² the carbonyl carbon is not detected at ambient temperature in ^{13}C NMR. The rate of interconversion between the π - and σ -isomers of **2** at ambient temperature is such that the CHO resonance is broadened into the base line. This CHO carbon can be detected at -80°C as a broad signal at 97.9 ppm that sharpens as the temperature is lowered to -95°C (CHO, 97.1 ppm). The downfield shift of nearly 100 ppm of the carbonyl carbon (CHO) of the σ -bound complex (**1**) compared to the chemical shift of the predominantly π -bound complex (**2**) observed at low temperatures indicates a rehybridization from sp^2 to sp^3 upon η^2 coordination to tungsten. The ^1H chemical shift of the aldehydic proton of **2** moves 0.36 ppm upfield as the temperature is lowered to -95°C (CHO, 6.79 ppm). Furthermore, complex **2** is thermochromic; the solution turns brown at lower temperatures, a color consistent with a π -bound $\text{TpW}(\text{CO})(\text{MeC}\equiv\text{CMe})^+$ aldehyde complex. These data suggest that **2** is predominantly a $\pi\text{-}p\text{-anisaldehyde}$ complex at low temperatures.

In order to change the spectroscopic time scale and probe the thermodynamic π/σ equilibrium without dynamic exchange complications, the temperature dependence of the π/σ equilibrium was assessed by infrared measurements.¹³ The 53:47 ($\pi:\sigma$) ratio at 21 °C increases to 74:26 at -42°C and to 94:6 at -78°C . A van't Hoff plot of these values ($\sigma \rightarrow \pi$) gave approximate ΔH° and ΔS° values of $-2.9 \text{ kcal mol}^{-1}$ ($-12.1 \text{ kJ mol}^{-1}$) and -9.6 eu ($-40.2 \text{ J K}^{-1} \text{ mol}^{-1}$), respectively. As expected, the π -isomer is favored enthalpically while the σ -isomer is favored entropically. The ΔG° values for this plot are -0.08 , -0.68 , and $-1.0 \text{ kcal mol}^{-1}$ for 21, -42 , and -78°C , respectively. Extrapolation from the plot predicts an estimated 24:1 ($\pi:\sigma$) ratio at -95°C . The significant shift in favor of the π -isomer of **2** at low temperatures explains why signals for the σ -isomer are not detected in low-temperature NMR spectra.

(9) Bochmann, M.; Webb, K. J.; Hursthouse, M. B.; Mazid, M. *J. Chem. Soc., Chem. Commun.* **1991**, 1735.

(10) For a structurally characterized cyclopentadienylmolybdenum π -benzaldehyde complex see: Brunner, H.; Wachter, J.; Bernal, I.; Creswick, M. *Angew. Chem., Int. Ed. Engl.* **1979**, *11*, 861.

(11) $[\text{TpW}(\text{CO})(\text{MeC}\equiv\text{CMe})(\eta^1/\eta^2\text{-}p\text{-O}=\text{CHC}_6\text{H}_4\text{OMe})][\text{BAR}'_4]$ (**2**): IR (CH_2Cl_2) $\nu_{\text{C}=\text{O}}$ 2030/1944 cm^{-1} ; ^1H NMR (250 MHz, CD_2Cl_2) δ 7.71 (br, 2 H of C_6H_4 partially obscured by $\sigma\text{-Hs}$ of BAR'_4), 7.15 (s, 1 H, CHO), 6.98 (br d, 2 H, $^3J_{\text{HH}} = 7.3 \text{ Hz}$, C_6H_4), 3.88 (s, 3 H, OMe), $^{13}\text{C}\{^1\text{H}\}$ NMR (400 MHz, CD_2Cl_2 , -95°C) δ 162.0 (C–OMe of C_6H_4), 130.2 (br, C_6H_4), 124.8 (*ipso* of C_6H_4), 124.0, 113.8, 113.1 (br, C_6H_4), 97.1 (br, CHO), 55.1 (OMe).

(12) Schuster, D. M.; White, P. S.; Templeton, J. L. Manuscript in preparation.

(13) A custom-made variable-temperature stop/flow IR cell designed by Dr. S. A. Evans, Jr., for use with a Mattson Galaxy 5000 FTIR was employed.

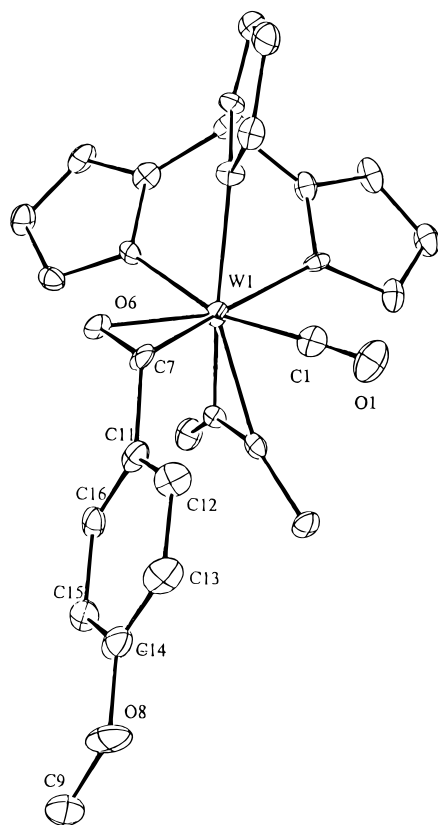


Figure 2. ORTEP diagram for $[\text{TpW}(\text{CO})(\text{MeC}\equiv\text{CMe})(\eta^2\text{-}p\text{-O}=\text{CHC}_6\text{H}_4\text{OMe})][\text{BAR}'_4] (\mathbf{2})$. Selected bond distances (Å) and angles (deg): W(1)–C(1), 1.964(12); W(1)–O(6), 1.974(6); W(1)–C(7), 2.268(11); C(1)–O(1), 1.196(14); O(6)–C(7), 1.308(14); C(7)–C(11), 1.484(15); C(11)–C(12), 1.420(16); C(12)–C(13), 1.385(17); C(13)–C(14), 1.368(18); C(14)–C(15), 1.413(16); C(15)–C(16), 1.394(15); C(16)–C(11), 1.355(16); C(14)–O(8), 1.362(14); O(8)–C(9), 1.418(16); C(7)–W(1)–C(1), 73.4(4); W(1)–C(7)–C(11), 125.9(7); W(1)–O(6)–C(7), 84.9(5); W(1)–C(7)–O(6), 60.1(5); O(6)–W(1)–C(7), 35.1(3); C(9)–O(8)–C(14)–C(13), -178.3 .

Workup of **2** gave orange crystals in 82% yield. The X-ray crystal structure of **2** reveals an octahedral coordination sphere with a π -bound *p*-anisaldehyde in the solid state (Figure 2). The solid-state geometry directs the aryl ring of the *p*-anisaldehyde ligand away from the bulky Tp ligand. The C(7)–C(11) bond forms a 25° angle with the W(1)–O(6)–C(7) plane. The C(7)–O(6) bond length of 1.308(14) Å is significantly longer

than the C=O bond length of **1** (1.237(7) Å), consistent with π -back-bonding from tungsten to the C=O π^* orbital of **2**. The C(7)–O(6) moiety of *p*-anisaldehyde is slipped¹⁴ substantially with respect to the tungsten metal center, with a W–O(6) bond length of 1.974(6) Å and a W–C(7) bond length of 2.268(11) Å. This W–C(7) bond distance is comparable to similar distances reported for related tungsten complexes.^{3d,15} The W–O(6) bond distance of 1.974(6) Å is surprisingly close to the W–OR bond distance of 1.971(6) Å observed in the $\text{Tp}^*\text{W}(\text{CO})(\text{PhC}\equiv\text{CMe})(\text{OCH}_2^t\text{Bu})$ alkoxide complex.^{3a} A torsion angle for C(9)–O(8)–C(14)–C(13) of -178.3° in **2** indicates a high degree of π -delocalization in the methoxyaryl unit.

This comparison study of molybdenum and tungsten demonstrates the dramatic effect of the metal on the preferred coordination mode of *p*-anisaldehyde. Stereochemical transformations of aldehydes and ketones bound to transition metals depend on their mode of coordination,^{3,16} and clearly the metal can exert a controlling influence in this regard.

Acknowledgment. We thank Dr. S. A. Evans, Jr., for use of his variable-temperature IR cell and Mattson Galaxy 5000 FTIR spectrometer. We thank Leila Telan of Dr. Evans' research group for assistance with the variable-temperature IR experiments. Generous support for this work was provided by the National Science Foundation (Grant No. CHE-9208207).

Supporting Information Available: Text giving experimental details and characterization data for the compounds listed in the text and listings of positional and thermal parameters, labeled figures, tables of all bond distances and angles, and tables of data collection parameters for **1** and **2** (24 pages). Ordering information is given on any current masthead page.

OM960869J

(14) (a) Eisenstein, O.; Hoffmann, R. *J. Am. Chem. Soc.* **1981**, *103*, 4308. (b) Cameron, A. D.; Smith, V. H., Jr.; Baird, M. C. *J. Chem. Soc., Dalton Trans.* **1988**, 1037.

(15) (a) Byran, J. C.; Mayer, J. M. *J. Am. Chem. Soc.* **1990**, *112*, 2298. (b) Chisholm, M. H.; Folting, K.; Klang, J. A. *Organometallics* **1990**, *9*, 607.

(16) (a) Duthaler, R. O.; Hafner, A. *Chem. Rev.* **1992**, *92*, 807. (b) Kagan, H. B.; Riant, O. *Chem. Rev.* **1992**, *92*, 1007. (c) Zassinovich, G.; Mestroni, G. *Chem. Rev.* **1992**, *92*, 1051. (d) Denmark, S. E.; Almstead, N. G. *Tetrahedron* **1992**, *48*, 5565. (e) Dalton, D. M.; Garner, C. M.; Fernández, J. M.; Gladysz, J. A. *J. Org. Chem.* **1991**, *56*, 6823. (f) Hill, J. E.; Fanwick, P. E.; Rothwell, I. P. *Organometallics* **1992**, *11*, 1771.